minerals

MDPI

Article

Migration Behavior of Lithium during Brine Evaporation and KCl Production Plants in Qarhan Salt Lake

Weijun Song [1,2], Hongze Gang [1], Yuanqing Ma [4], Shizhong Yang [1] and Bozhong Mu [1,3,*]

1 Key Laboratory of Bioreactor Engineering and Institute of Applied Chemistry, East China University of Science and Technology, Shanghai 200237, China; wjsong@mail.ecust.edu.cn (W.S.); ganghz@ecust.edu.cn (H.G.); meor@ecust.edu.cn (S.Y.)
2 School of Chemical Engineering, Qinghai University, Xining 810016, China
3 Shanghai Collaborative Innovation Center for Biomanufacturing Technology, Shanghai 200237, China
4 Qinghai Salt Lake Industry Group Co. Ltd., Golmud 816000, China; yhjfmyq@gmail.com
* Correspondence: bzmu@ecust.edu.cn

Academic Editor: Javier Sánchez-España
Received: 8 January 2017; Accepted: 2 April 2017; Published: 11 April 2017

Abstract: Lithium-brine is an important potential source of lithium. Much research and investigation has been carried out aimed at lithium recovery from brine. Although the distribution and occurrence status of lithium in brine have important implications for lithium recovery, few reports had correlated to this issue. In this article, a study was carried out to explore the lithium migration behavior during brine evaporation and KCl production process at Qarhan Salt Lake. The occurrence status of lithium both in fresh mined brine and residual brine after evaporation were also speculated by means of lithium concentration evaluation and theoretical calculation based on the Pitzer electrolyte solution theory. Results showed that, for Qarhan brine mined from the Bieletan region, most lithium was enriched in the residual brine during the brine evaporation process. The concentration of lithium in the residual brine could be more than 400 mg/L. More than 99.93% lithium ions in residual brine exist in free ions state and lithium does not precipitate from brine with a density of 1.3649 g/mL. The results also revealed that lithium concentration in wastewater discharged from KCl plants can reach a level of 243.8 mg/L. The investigation results provide a theoretical basis for comprehensive development and utilization of lithium resources in Qarhan Salt Lake.

Keywords: lithium migration; occurrence status; Qarhan Salt Lake

1. Introduction

As an energy metal of the twenty-first century, lithium had attracted more and more attention in the past few decades. Lithium has been widely applied in high energy batteries, controlled thermonuclear reactions, the manufacturing of ceramic and glass, and other fields [1–7]. Lithium consumption for batteries had increased most significantly due to the development of the electric vehicle industry and the popularity of portable electronic products. Stimulated by the political affairs, economic requirements, and environmental conservation, lithium resources have become the focus of the international mining market and lithium's position as a strategic resource is becoming more prominent.

Salt lake brine, thermal spring, and oilfield water are important geological sources of lithium. The commercial exploitation of the lithium resource of brine began at the Searles Lake in the US in 1936. Since then, more focus has been placed on recovering lithium from salt lake brine because of its low economical cost and low environmental impact [8–10]. As a country possessing huge

amount of brine, China accounts for one-third of the world's liquid lithium reserves. In China, most lithium-rich lakes are located in the Qinghai-Tibet plateau. Among them, Qarhan Salt Lake is the biggest playa lake containing huge lithium reserves of 1.64 Mt. Qarhan has promising research value and development prospects of lithium resource in the near future [4,5,11–13]. Despite relevant research on recovering lithium from salt lakes brine having been undertaken since 1970s, currently most of these studies concern lithium distribution during the brine evaporation process focusing on the two types of brine: carbonate-type brine with high lithium concentration, such as Zabuye Salt Lake brine in which concentration of lithium was 1085–1848 mg/L [12] and lithium always precipitate from aqueous in the form of carbonate as brine evaporates [13,14]; and the $NaSO_4$ subtype brine with high lithium concentration such as Zhacang kaca Salt Lake (lithium concentration was 1210–2303 mg/L) [15] and East TaiJanier Salt Lake (543–1496 mg/L) [16]. In this type of brine, lithium will precipitate from solution in the form of sulfate as brine evaporates [15,17]. For the types of brine described above, lithium recovery is relatively easy due to the high concentration and less disturbance of magnesium. However, the studies focusing on the lithium behavior during evaporation process, for $MgSO_4$ subtype brine such as Qarhan Salt Lake brine, are limited and the knowledge on lithium occurrence in this type of brine is rare.

Therefore, the aim of this paper was to investigate and compare the lithium concentration level of Qarhan Salt Lake brine during the process of natural evaporation in order to fully characterize the migration and occurrence status of lithium and hoping to supply some theoretical basis on utilization of lithium resources in the Qarhan Salt Lake. Since the Qarhan Salt Lake not only has huge lithium development potential but also was the biggest KCl base in China, for the purpose of improving the brine utilization rate, lithium can be recovered from brine as a co-product in the fabrication of KCl. The plan is to contribute to the data from the KCl production line at Qarhan Salt Lake in order to fill the gap of information on lithium distribution in the KCl plant. Additionally, to develop lithium resource in a long range, the lithium geographical distribution of whole of the Qarhan Salt Lake was also summarized.

2. Materials and Methods

The field samples were taken from the salt ponds and KCl plants of the Qinghai Salt Lake Industry Group Co. at Qarhan. The original brine, both in simulation experiments and field sampling, refers to the brine taken from the entrance of salt pond (Site a) as shown in Figure 1. Field samples from salt ponds were taken according to the sequence of salt crystallization and the brine flow direction. A total of eight solid samples and eight liquid samples were collected from different salt ponds locations, and seven solid samples and 11 liquid samples were collected from KCl plants. For each location, solid samples were collected into wide mouth polyethylene bottles, sealed with sealing tape immediately, and then brought back for lab testing. The liquid samples were collected in polyethylene bottles after rinsing the bottles three times. Liquid samples were centrifuged (3000 rpm) for two minutes to remove sediments and acidized with trace-metal HNO_3. The solid samples were suction filtrated to remove brine on their surface, dissolved using ultra-high purity water and acidized with trace-metal HNO_3. Samples collected in flotation stage were treated after de-foaming naturally. The cations (Li^+, K^+, Na^+, Mg^{2+}) in all samples were analyzed using inductively coupled plasma atomic emission spectrometer (ICP-AES, ICAP6300, Thermo Fisher, Waltham, MA, USA) and $SO_4{}^{2-}$ was determined by gravimetric analysis. Brine density was measured by the method of pycnometer and the solid phase was identified by X-ray diffraction (XRD, Goniometer RINT2000, Rigaku, Akishima, Japan).

Lithium distribution both in solid and liquid phase at different evaporation stages were investigated both in labor and production sites by means of simulation experiments and field sampling. The simulation experiment was carried out in a transparent plastic container, placed outside in natural conditions. Brine was evaporated in the sun at Xining, Qinghai (altitude: 2290 m, atmospheric pressure: 77.273 kPa). Fixed time was assign to observe the brine evaporation degree every day, including temperature, brine temperature, brine depth, density, and crystallization of salt precipitation.

In the process, solid and liquid samples were separated by filtration and for chemical analysis. After the solid-liquid separation was carried out, the evaporation and crystallization were continued.

3. Results and Discussion

3.1. Lithium Distribution in Qarhan Salt Lake

A large dry salt plain and 10 varying sized brine lakes constitutes the present terrain of the Qarhan Salt Lake, which is 168 km long from east to west and varies in width from 20~40 km. The Qarhan Salt Lake can be divided into four main regions from east to west: the Huobuxun region, the Qarhan region, the Dabuxun region, and the Bieletan region, as shown in Figure 1. Interstitial brine was mined in the Bieletan region and then transported by collection trenches to salt ponds. Brine was evaporated in these ponds to crystallize carnallite for KCl production. The entrance of the salt pond (Site a) is about 28 km away from the Bieletan region. In order to reduce costs and increase energy saving, brine flow was only driven by its gravitational potential and no extra power was supplied during transportation. After long distance transportation in open-air, brine composition changes and differs from its initial state.

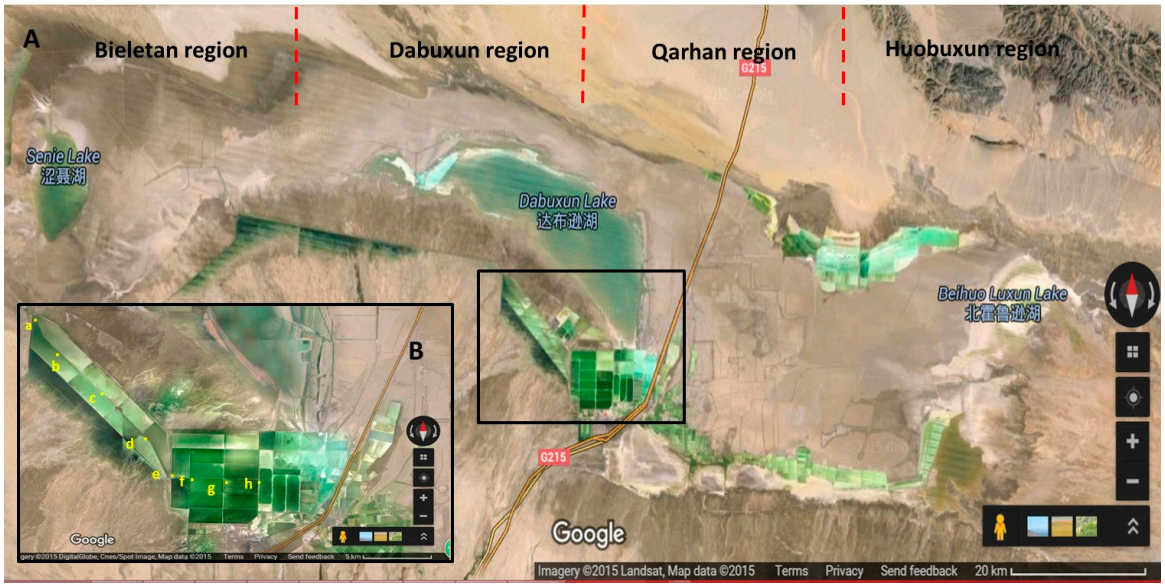

Figure 1. (**A**) Qarhan Salt Lake ichnography; (**B**) Detail of salt pond in the Salt Lake Group. The sampling site in evaporation precess was presented by yellow dots. (a: source brine; b: NaCl pond 1; c: NaCl pond 2; d: brine adjusting pond; e: carnallite pond 1; f: carnallite pond 2; g: carnallite pond 3; h: residue brine pond).

The lithium concentration value in the different regions of whole Qarhan Salt Lake is listed in Table 1. Based on Figure 1, lithium resource distribution in the Qarhan Salt Lake presented a regional feature: lithium gradient concentration of brine increased from east to west, south to north. Bieletan region, the northwest edge of the Qarhan Salt Lake presented the highest lithium concentration level.

Table 1. Lithium concentration and the magnesium-lithium ratio of the Qarhan Salt Lake.

Lake Name	Water Type	pH	Salinity (g/L)	Mg^{2+} (g/L)	Li^{+} (mg/L)	$[Mg^{2+}]/[Li^{+}]$
Huobuxun	Interstitial brine	6.70	311.2	21.19	10.3	2057.76
Huobuxun (N)	Surface brine	-	306.8	7.74	88.4	87.55
Huobuxun (S)	Surface brine	6.70	346.1	19.71	19.6	1004.08
Tuanjie	Surface brine	5.40	425.3	98.69	59.0	1672.71
Xiezuo	Surface brine	5.50	358.5	64.69	28.6	226.18
Qarhan	Interstitial brine	7.00	321.1	28.67	15.6	1837.63
Dabuxun	Surface brine	5.32	307.2–470.2	118.69	88.4	1342.65
Dabuxun	Interstitial brine	6.70	331.8	46.54	26.0	1789.96
Bieletan	Interstitial brine	6.50	358.0	64.15	124.0	517.34
Bieletan	Subsurface brine	-	289.0–470.1	9.76–109.7	90.0–1225.0	100–200
Xiao Biele	Surface brine	6.2	386.9	81.57	66.3	1230.34
Da Biele	Surface brine	7.0	362.9	30.99	37.0	837.57
Senie	Surface brine	7.1	332.3	18.12	191.0	94.87

Data source: Reference [18].

The average lithium concentration in the Bieletan region was 594 mg/L and the maximum value even could reach 1.225 g/L, which was almost comparable to the East TaiJanier area. Thus, the Bieletan could also be a region with the highest lithium concentration in the whole Qaidam basin. In the Dabuxun region, the average lithium concentration of interstitial brine was 26.0 mg/L, while it was 88.4 mg/L in the surface brine. This could be because lithium is highly soluble and did not readily produce evaporate minerals when concentrated by evaporation. Lithium would rather stay in residual brines in the surface or shallow subsurface. The lithium concentration of the Huobuxun region was the lowest in the whole Qarhan Salt Lake (only 10.3 mg/L) and its brine magnesium-lithium ratio was more than 2000, too high to recover lithium [10,19]. Since the brine of the Qarhan Salt Lake belongs to the magnesium sulfate subtype, it usually contains high magnesium as shown in Table 1. According to the boundary grade of industrial development, the concentration of lithium in brine should be approximately 25 mg/L. Thus, the brine collected from west of the Qarhan region (such as in the Bieletan and Dabuxun regions) has the potential for lithium exploitation.

3.2. Distribution of Lithium during the Evaporation Process at Salt Ponds

Figure 2 shows lithium distribution during brine evaporation process in both the simulation experiment and field sampling from different salt ponds. As brine concentrating lithium in aqueous phase was enrichened, the average concentration of lithium could reach a level of 500 mg/L. In residual brine, this was more than double the concentration in the original brine. The simulation experiments showed that the vast majority of lithium was retained in the aqueous phase and there was a positive correlation between lithium concentrations with brine enrichment degree.

Lithium content in solid phase had no evident change ($p > 0.05$) during the brine concentration process until bischofite was precipitated. Although brine was more concentrated by natural evaporation, lithium did not saturated or form its own minerals until brine flowed into the residual brine pond. Even the highest mass percent of lithium in solid phase was less than 0.004% and could be ignored. Thus, the solid phase containing lithium mainly was the result of parent brine entrainment. When bischofite began to precipitate, lithium content in the solid phase increased slightly because the lithium isomorphically substitutes magnesium in bischofite. Additionally, the solid identification results shown in Table 2 also confirm that lithium salt was unformed during the whole evaporation process.

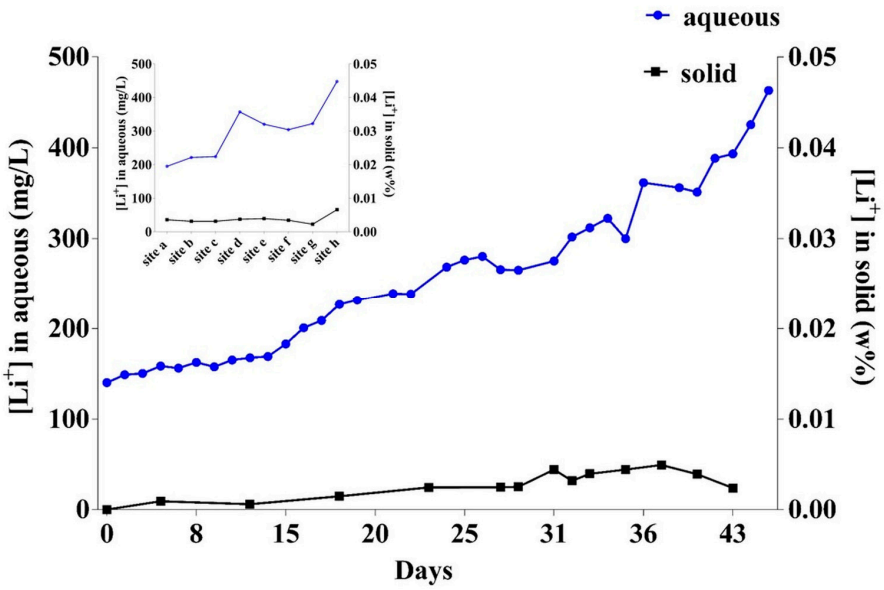

Figure 2. Lithium distribution during the brine evaporation process.

Table 2. Identification results of solid phase during the brine evaporation process.

Density (g/cm^3)	Halite (%)	Bischofite (%)	Carnallite (%)
1.2602	95	5	0
1.2768	94	6	0
1.2944	44	7	49
1.3218	24	5	71
1.3373	24	8	68
1.3559	70	0	30
1.3579	2	85	13
1.3634	0	100	0
1.3648	0	100	0
1.3654	0	100	0
1.3668	0	100	0
1.3891	1	99	0
1.3692	0	100	0

The relationship of magnesium-lithium ratio between brine densities during the evaporation process is given in Figure 3. It shows that the Magnesium-lithium ratio does not changed much in early evaporation stage (depicted in magenta and violet colors), but a larger change appears when the brine density value is more than 1.285 g/cm^3 (depicted in blue and green colors). The magnesium-lithium ratio decreases sharply in the later stage of evaporation, especially when brine density is more than 1.345 g/cm^3. Brine magnesium-lithium ratio decreases almost to half of initial value when the brine density is around 1.372 g/cm^3 (depicted in red).

The brine density value could represent the degree of brine concentration because brine density is proportional to the degree of evaporation. The greater the density value, the higher the degree of brine evaporation and lithium enrichment. As shown in Figure 3, the magnesium-lithium ratio remains at about the same level in the early evaporation stage, but a slight decrease appears when the brine density value is more than 1.28 g/cm^3, almost the moment when carnallite crystalized. Thus, it can be deduced that the brine magnesium-lithium ratio decrease was caused by carnallite precipitation. This is because carnallite is a double salt that contains 8.64% magnesium and the precipitation led the magnesium ions to migrate to solid from aqueous. The magnesium-lithium ratio decreased sharply in the later stage of evaporation, especially when brine density was more than 1.34. The brine magnesium-lithium ratio value almost decreased half of its original value when the brine density reached 1.37 g/L. However,

at this time, the mineralization degree of brine was too high for rapid evaporation. Such a high salinity could significantly decrease the water saturated vapor pressure on the top of the solution and lead to a slow evaporation. Furthermore, at this time the brine surface would be covered by a layer of salt crystal that could block the diffusion of water molecules to the outside. It would be time-consuming to decrease the brine magnesium-lithium ratio through continue evaporation. Continue evaporation brine requires huge place to build a salt pan, thus it is very uneconomical to decrease magnesium-lithium ratio by sustained evaporation for industrial production.

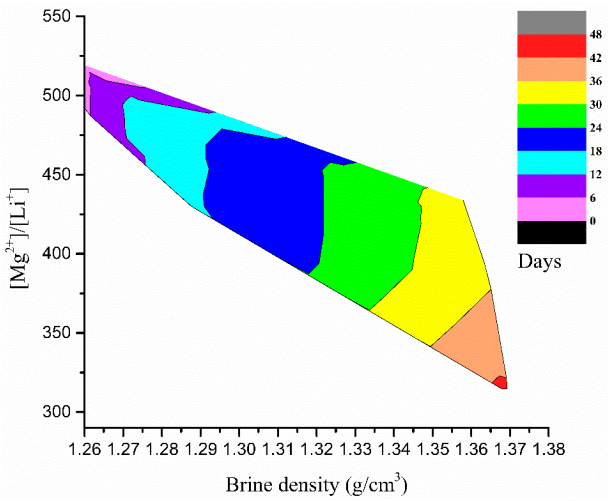

Figure 3. The variation tendency of magnesium-lithium ratio during evaporation process. Time course of brine evaporation is represented by different colors. The size of the area has a positive correlation with density and $[Mg^{2+}]/[Li^{+}]$.

3.3. Lithium Occurrence Status during Brine Evaporation

A chemical model for sea water was presented by Garrels to assess the percentages of the major dissolved species [20], however, due to the super high ionic strength of brine, it is inapplicable to use this model into salt lake brine system without parameter correction. In the 1980s, Harive and Wear recompiled the Pitzer electrolyte thermodynamic calculation formula [21,22] as follows:

$$\begin{aligned}\phi - 1 = {} & \left(\sum_i m_i\right)^{-1}\left\{2\left[-\frac{A^{\phi} I^{\frac{3}{2}}}{\left(1+1.2I^{\frac{1}{2}}\right)} + \sum_{i_c=1}^{N_c}\sum_{i_A=1}^{N_A} m_c m_A\left(B^{\phi}_{cA} + ZC_{cA}\right)\right]\right. \\ & + \sum_{i_c=1}^{N_c-1}\sum_{j_A=i_c+1}^{N_c} m_c m_{c'}\left(\Phi^{\phi}_{cc'} + \sum_{i_A=1}^{Nc} m_A \psi_{cc'A}\right) \\ & + \sum_{i_c=1}^{N_A-1}\sum_{j_N=i_A+1}^{N_A} m_A m_{A'}\left(\Phi^{\phi}_{AA'} + \sum_{j_c=1}^{N_c} m_c \psi_{Ac'c} + \sum_{i_N=1}^{N_N}\sum_{j_A=1}^{N_A} m_N m_A \lambda_{NA}\right. \\ & \left.\left. + \sum_{i_N=1}^{N_N}\sum_{j_c=1}^{N_c} m_N m_c \lambda_{Nc}\right)\right\}\end{aligned} \tag{1}$$

$$\begin{aligned}\ln \gamma_M = {} & Z_M^2 \\ & + \sum_{i_A=1}^{N_A} m_A(2B_{MA} + ZC_{MA}) \\ & + \sum_{i_c=1}^{N_A} m_c\left(2\Phi_{Mc} + \sum_{i_A=1}^{N_A} m_A \psi_{McA}\right) + \sum_{i_A=1}^{N_A-1}\sum_{j_{A'}+1}^{N_A} m_A m_{A'} \psi_{AA'M} \\ & + |Z_M| \sum_{i_c=1}^{N_c}\sum_{i_A=1}^{N_A} m_c m_A C_{cA} + \sum_{i_N=1}^{N_N} m_N(2\lambda_{NM})\end{aligned} \tag{2}$$

$$\begin{aligned}\ln\gamma_X = {} & Z_X^2 F \\ & + \sum_{i_c=1}^{N_A} m_c(2B_{cX} + ZC_{cX}) \\ & + \sum_{i_A=1}^{N_A} m_A\left(2\Phi_{XA} + \sum_{i_c=1}^{N_A} m_c\psi_{XcA}\right) + \sum_{i_c=1}^{N_{c-1}}\sum_{j_{c'}=i_c+1}^{N_A} m_c m_{c'}\psi_{cc'M} \\ & + |Z_X|\sum_{i_c=1}^{N_c}\sum_{i_A=1}^{N_A} m_c m_A C_{cA} + \sum_{i_N=1}^{N_N} m_N(2\lambda_{NX})\end{aligned} \tag{3}$$

$$\ln\gamma_N = \sum_{i_c=1}^{N_c} m_c(2\lambda_{Ac}) + \sum_{i_A=1}^{N_A} m_A(2\lambda_{NA}) \tag{4}$$

In the above formulas: I for ion strength, A^ϕ for Debye-Hükel coefficient. M, c, and c' for cations, X, A, and A' for anions, m_c for molality of cation, Z_c for charge number of cation, and N_c for the species number of cations. The anions A and neutral molecule N can be defined in same manner. The functions of F, C, Z, A^ϕ, ψ, Φ, B^ϕ, and B was defined as follows:

$$\begin{aligned}F = -A^\phi\Bigg[& \frac{I^{\frac{1}{2}}}{\left(1+1.2I^{\frac{1}{2}}\right)} + \frac{2\ln\left(1+1.2I^{\frac{1}{2}}\right)}{1.2} + \sum_{i_c=1}^{N_c}\sum_{i_A=1}^{N_A} m_c m_A B'_{cA} \\ & + \sum_{i_c=1}^{N_c}\sum_{i_{c'}=i_c+1}^{N_c} m_c m_{c'}\Phi'_{cc'} + \sum_{i_A=1}^{N_A}\sum_{i_A=i_A+1}^{N_A} m_A m_{A'}\Phi'_{AA'}\Bigg]\end{aligned} \tag{5}$$

$$C_{MX} = \frac{C^\phi_{MX}}{\left(2|Z_M Z_X|^{\frac{1}{2}}\right)} \tag{6}$$

$$Z = \sum_i |Z_i| M_i \tag{7}$$

$$B^\phi_{cA} = \beta^{(0)}_{cA} + \beta^{(1)}_{cA}\exp\left(-\alpha_1 I^{\frac{1}{2}}\right) + \beta^{(2)}_{cA}\exp\left(-\alpha_2 I^{\frac{1}{2}}\right) \tag{8}$$

$$B_{cA} = \beta^{(0)}_{cA} + \beta^{(1)}_{cA}\mathrm{g}\left(\alpha_1 I^{\frac{1}{2}}\right) + \beta^{(2)}_{cA}\mathrm{g}\left(\alpha_2 I^{\frac{1}{2}}\right) \tag{9}$$

$$B'_{cA} = \left[\beta^{(1)}_{cA}\,\mathrm{g}'\left(\alpha_1 I^{\frac{1}{2}}\right) + \beta^{(2)}_{cA}\,\mathrm{g}'\left(\alpha_2 I^{\frac{1}{2}}\right)\right]/I \tag{10}$$

$$\mathrm{g}(x) = 2[1-(1+x)\exp(-x)]/x^2 \tag{11}$$

$$\mathrm{g}'(x) = -2\left[1-\left(1+x+\frac{x^2}{2}\right)\exp(-x)\right]/x^2 \tag{12}$$

α_1 = 2.0 $\mathrm{kg}^{1/2}$ $\mathrm{mol}^{-1/2}$ and α_2 = 0 for the electrolyte solution which contains at least one monovalent ion; α_1 = 1.4 $\mathrm{kg}^{1/2}$ $\mathrm{mol}^{-1/2}$ and α_2 = 12 $\mathrm{kg}^{1/2}$ $\mathrm{mol}^{-1/2}$ for the electrolyte solution in which anions and cations were both divalent.

$$\Phi^\Phi_{ij} = \theta_{ij} + E_{\theta_{ij}} + IE_{\theta'_{ij}} \tag{13}$$

$$\Phi_{ij} = \phi_{ij} + E_{\theta_{ij}} \tag{14}$$

$$\Phi'_{ij} = E_{\theta'_{ij}} \tag{15}$$

If the suitable Pitzer parameters were available, then the osmotic coefficient and the ionic activity coefficient for each species in the system of high concentration mixed electrolyte solution could be calculated by the H-W equation. Song and Yan [23] presented the mixing Pitzer parameters for lithium brine system in 2003. Thus, the procedures was to find the proper thermodynamic parameters of the

Pitzer model for the Li^+, Na^+, K^+, Mg^{2+}/Cl^-, SO_4^{2-} brine system and use them to calculate individual ion activity coefficients values. Then, according to the coefficient values of each ion and dissociation constants, the percentages of all species can be obtained simultaneously. In this work, the individual ion activity coefficients were calculated by H-W equation and the parameters used in the equation are listed in Tables 3 and 4.

Table 3. Pitzer parameters of the single electrolyte used in the chemical model of the Qarhan brine system.

Cation	Anion	$\beta^{(0)}$	$\beta^{(1)}$	$\beta^{(2)}$	$C^{(\phi)}$	Reference
Na^+	Cl^-	0.0765	0.2664	-	0.00127	[21]
Na^+	SO_4^{2-}	0.01958	1.113	-	0.00497	[21]
K^+	Cl^-	0.04835	0.2122	-	−0.00084	[21]
K^+	SO_4^{2-}	0.04995	0.7793	-	-	[21]
Mg^{2+}	Cl^-	0.35235	1.6815	-	0.00519	[21]
Mg^{2+}	SO_4^{2-}	0.2210	3.343	−37.23	0.025	[21]
Li^+	Cl^-	0.20818	−0.07264	-	−0.004241	[23]
Li^+	SO_4^{2-}	0.14396	1.17736	-	−0.05710	[23]

Table 4. Mix Pitzer parameters used in the chemical model of the Qarhan brine system.

Parameter	Value	Reference	Parameter	Value	Reference
$\theta_{Na,Li}$	0.02016	[23]	Φ_{Na,Li,SO_4}	−0.00600	[23]
$\theta_{Na,Mg}$	0.07000	[21]	Φ_{Na,K,SO_4}	-	[21]
$\theta_{Na,K}$	−0.01200	[21]	$\Phi_{Na,K,Cl}$	−0.007416	[21]
$\theta_{K,Li}$	−0.05075	[21]	$\Phi_{Na,Mg,Cl}$	−0.007774	[21]
$\theta_{K,Mg}$	0.00000	[21]	Φ_{Na,Mg,SO_4}	−0.01000	[21]
$\theta_{Mg,Li}$	0.010196	[21]	Φ_{K,Li,SO_4}	−0.00180	[21]
θ_{Cl,SO_4}	0.02000	[21]	$\Phi_{K,Li,Cl}$	−0.01200	[21]
$\Phi_{Cl,SO_4,Li}$	−0.01236	[23]	Φ_{K,Mg,SO_4}	−0.01500	[23]
$\Phi_{Cl,SO_4,Na}$	0.001400	[21]	$\Phi_{K,Mg,Cl}$	−0.00797	[21]
$\Phi_{Cl,SO_4,Mg}$	−0.04800	[21]	$\Phi_{Mg,Li,Cl}$	−0.005909	[23]
$\Phi_{Cl,SO_4,K}$	−0.02200	[21]	Φ_{Mg,Li,SO_4}	−0.0005947	[23]
$\Phi_{Na,Li,Cl}$	0.005700	[23]	-	-	-

The chemical composition and calculation activity coefficient of individual ion in the Qarhan Salt Lake brine before and after evaporation are shown in Table 5. Superscript "O" and "R" represent the original brine and the residual brine after evaporation.

Table 5. Chemical composition and activity coefficient of the Qarhan Salt Lake, 25 °C.

Ions	Li^+	Na^+	K^+	Mg^{2+}	Cl^-	SO_4^{2-}
Molality (mol/Kg)^O	0.0247	1.1242	0.4446	3.9029	8.5914	0.4040
Activity coefficient	3.4639	1.0991	0.2741	4.0269	7.3692	0.0146
Molality (mol/Kg)^R	0.0607	0.0902	0.0201	6.5376	10.4158	1.4151
Activity coefficient	2.9457	1.6503	0.1735	14.4273	33.0842	0.0132

The chloride ion was generally believed not to form ion pairs with alkali metal and alkaline earth metal ions. It is still assumed that chloride ions do not form ion pairs when applying the chemical model to dealing with the Qarhan lithium-brine system. According to the Qarhan Salt Lake brine, sulfate can be considered in the calculation process. Thus, for lithium, two equations can be obtained as follows:

$$m_{Li^+_{Totall}} = m_{Li^+_{Free}} + m_{(Li-SO_4^{2-})^-} \quad (16)$$

$$\frac{\gamma_{Li^+} m_{Li^+} \times \gamma_{SO_4^{2-}} m_{SO_4^{2-}}}{\gamma_{LiSO_4^-} m_{LiSO_4^-}} = K_{diss} \quad (17)$$

The dissociation constant and activity coefficient of ion-pairs are listed in Table 6. The rest of the ions were processed in the same way as lithium, then a series of equations can be obtained. The proportion of the free ion and the ion pair for major dissolved species can be calculated by solving these equations (for a detailed process, see Reference [19]).

Table 6. The dissociation constant of major dissolved species and activity coefficient of ion-pairs.

Species	**Na_2SO_4**	**K_2SO_4**	**$MgSO_4$**	**Li_2SO_4**	**Reference**
Dissociation constant	0.190546	0.109648	0.004365	0.640000	[20,24]
Ion–pairs	**Na–SO_4**	**K–SO_4**	**Mg–SO_4**	**Li–SO_4**	**Reference**
Activity coefficient	0.63000	0.63000	1.13000	0.63000	[22,25]

A summary value, the proportion of the free ion and the ion pair for major dissolved species in the Qarhan Salt Lake, is shown in Table 7. The calculation results show that the vast majority of lithium occurrence are free ions in brine during the whole evaporation process. There was a slight decrease in the percentage value of lithium ion-pair as the brine evaporated. The percent value of Li-SO_4 in residue brine was just 0.02% lower than the original brine. Only magnesium ions are significant combined into ion pairs, and the other alkali metal ions are not conspicuous. Comparing the percentage value of lithium ion-pair in the Qarhan Salt Lake with East TaiJanier [21], it was found that lithium in the brine of the Qarhan Salt Lake was more likely to occur as free ions. This could be due to the higher concentration of magnesium in brine and the stronger combination trend between magnesium and sulfate.

Table 7. Occurrence state of major dissolved species before and after brine evaporation at 25 °C.

Ion	**Original Brine**		**Residue Brine**	
	Occurrence Status	**Percent**	**Occurrence Status**	**Percent**
K^+	Free ion K-SO_4	99.946% 0.054%	Free ion K-SO_4	99.976% 0.024%
Li^+	Free ion Li-SO_4	99.911% 0.089%	Free ion Li-SO_4	99.931% 0.069%
Mg^{2+}	Free ion Mg-SO_4	89.931% 10.069%	Free ion Mg-SO_4	78.463% 21.573%
Na^+	Free ion Na-SO_4	99.874% 0.126%	Free ion Na-SO_4	99.818% 0.182%
SO_4^{2-}	K-SO_4 Li-SO_4 Mg-SO_4 Na-SO_4 Free ion	0.060% 0.005% 97.277% 0.350% 2.327%	K-SO_4 Li-SO_4 Mg-SO_4 Na-SO_4 Free ion	- - 99.500% 0.001% 0.4999%

3.4. Distribution of Lithium at the KCl Production Plants

Since another aim of this study was to contribute lithium distribution information in the whole KCl production line for recovering lithium from brine as a co-product of KCl, lithium distribution in KCl plants should also be taken into account. Figure 4 is the flow chart of KCl production in plant. The feed material of KCl production at plants was carnallite, which could be obtained after brine evaporation. When crude carnallite is taken out of the carnallite ponds, it is usually in a state of liquid-solid mixture and is always mixed with about 20% sodium chloride (NaCl), which needs to be

removed before producing KCl. Furthermore, the crude carnallite mined from carnallite pond often mixes with a lot of brine. A huge thickener was used to remove redundant brine to meet flotation specifications. Hence, in production operations, NaCl was reverse flotation from carnallite, first using alkyl-morpholine as a collector, then the treated carnallite with a low NaCl content (less than 5%) was decomposed and recrystallized in a crystallizer to produce KCl. The KCl from the crystallizer was centrifuged and dried for packing after filtered.

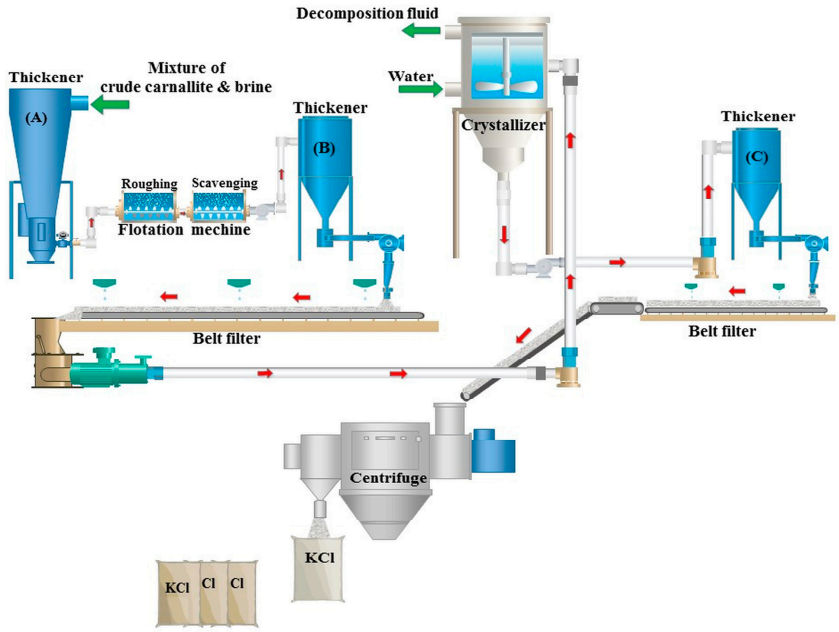

Figure 4. Flow chart of KCl production in plant.

Figure 5 illustrated the lithium distribution in KCl plant. According to the situation in plants, the maximum lithium content values for samples were 400 mg/L in aqueous phase and 0.005% in solid phase.

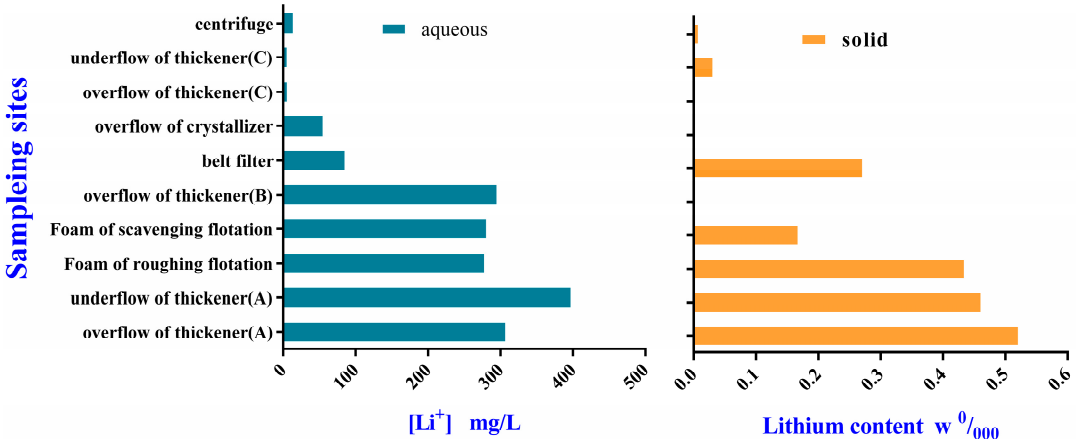

Figure 5. The distribution of lithium at KCl production plant.

As shown in Figure 5, in the aqueous phase of thickener A, although average lithium concentration in aqueous almost has same level with the brine of the carnallite pond, there were still some differences in lithium concentration between the overflow and underflow. The lithium concentration in the underflow being higher than the overflow might be caused by higher solid content in the underflow.

The survey showed that solid lithium content of the scavenging flotation foam phase would have an obvious decrease compared with the roughing flotation foam phase. However, the reasons for this phenomenon are not very clear and there is little research reported on it. After the first de-brine, the sharp decrease in the content of lithium in both the aqueous and solid phases could be due to drip washing: to meet purity specifications of final KCl, the easy soluble ions absorbed on the surface of carnallite, such as lithium and magnesium, are always removed by drip washing in the de-brine process. Based on the information in Figure 5, it is speculated that in plants, most lithium was dissolved and discharged with wastewater. Then the lithium concentration in the wastewater pond from KCl plants was detected and it was found that the lithium concentration could reach a level of 243.8 mg/L. This confirms the speculation and means besides the residual brine in evaporation process, the wastewater in the KCl plants also should be fully used to recovered lithium as a co-production of KCl.

4. Conclusions

In summary, the investigation came to the following conclusions: (1) the brine collected from west of the Qarhan region such as in the Bieletan and Dabuxun regions, is a prospective source for lithium exploitation. (2) Based on the results from simulation experiments and field sampling (both the salt pond in open air and the KCl plant), it is reasonable to believe that most of the lithium was enriched in the residue brine after carnallite precipitation. The residue brine and wastewater from the KCl plants should be used for lithium recovery. (3) More than 99.6% of the lithium ions in the liquid phase of the Qarhan Salt Lake occurred in the form of free ions, and the lithium ions did not precipitate because the brine was concentrated to a density of 1.3649 g/cm^3.

Acknowledgments: This research was supported in by the National Natural Science Foundation of China (U1507122, 21266027) and the Natural Science Foundation of Qinghai Province, 2016-ZJ-734. The authors also thank Sheng-Tai Zhang (Qinghai Salt Lake Industry Group Co.) for help with specimen collection.

Author Contributions: Bozhong Mu and Weijun Song designed the experiments. Weijun Song carried out the samples analysis. Yuanqin Ma and Weijun Song collected the samples and did the preliminary analysis. Hongze Gang and Shizhong Yang provided suggestions for the experiments and results analysis. Weijun Song prepared the manuscript with contributions from all co-authors.

Conflicts of Interest: The authors declare no conflict of interest.

References

1. Gruber, P.W.; Medina, P.A.; Keoleian, G.A.; Kesler, S.E.; Everson, M.P.; Wallington, T.J. Global Lithium Availability. *J. Ind. Ecol.* **2011**, *15*, 760–775. [CrossRef]
2. Kesler, S.E.; Gruber, P.W.; Medina, P.A.; Keoleian, G.A.; Everson, M.P.; Wallington, T.J. Global lithium resources: Relative importance of pegmatite, brine and other deposits. *Ore Geol. Rev.* **2012**, *48*, 55–69. [CrossRef]
3. Scrosati, B.; Garche, J. Lithium batteries: Status, prospects and future. *J. Power Sources* **2010**, *195*, 2419–2430. [CrossRef]
4. Song, P.S.; Xiang, R.J. Utilization and exploitation of lithium resources in salt lakes and some suggestions concerning development of Li industries in China. *Miner. Depos.* **2014**, *33*, 977–992.
5. Nie, Z.; Bu, L.Z.; Liu, J.H.; Wang, Y.S.; Zheng, M.P. Status of potash resources in salt lakes and progress in potash technologies in China. *Acta Geosci. Sin.* **2010**, *31*, 869–874.
6. Will, F.G. Impact of lithium abundance and cost on electric vehicle battery applications. *J. Power Sources* **1996**, *63*, 23–26. [CrossRef]
7. Tarascon, J.M.; Armand, M. Issues and challenges facing rechargeable lithium batteries. *Nature* **2001**, *414*, 359–367. [CrossRef] [PubMed]
8. Somrani, A.; Hamzaoui, A.H.; Pontie, M. Study on lithium separation from salt lake brines by nanofiltration (NF) and low pressure reverse osmosis (LPRO). *Desalination* **2013**, *317*, 184–192. [CrossRef]
9. Xiao, G.P.; Tong, K.F.; Zhou, L.S.; Xiao, J.L.; Sun, S.Y.; Li, P.; Yu, J.G. Adsorption and desorption behavior of lithium ion in spherical PVC–MnO_2 ion sieve. *Ind. Eng. Chem. Res.* **2012**, *51*, 10921–10929. [CrossRef]
10. An, J.W.; Kang, D.J.; Tran, K.T.; Kim, M.J.; Lim, T.; Tran, T. Recovery of lithium from Uyuni salar brine. *Hydrometallurgy* **2012**, *117*, 64–70. [CrossRef]

11. Zheng, X. Distribution characteristics of boron and lithium in brine of Zhacang Caka salt lake, Xizang (Tibet), China. *Chin. J. Oceanol. Limnol.* **1984**, *2*, 218–227.
12. Dong, T.; Tan, H.; Zhang, W.; Zhang, Y. Geochemical distribution of lithium in saline lakes in Tibet. *J. Hohai Univ. Nat. Sci.* **2015**, *43*, 230–235.
13. Nie, Z.; Bu, L.Z.; Zheng, M.P. Lithium resources industrialization of salt lakes in China: A case study of the Xitaijinaier Salt Lake and the Zabuye Salt Lake. *Acta Geosci. Sin.* **2010**, *31*, 95–101.
14. Zheng, M.P.; Zhang, Y.S.; Liu, X.F.; Qi, W.; Kong, F.J. Progress and prospects of salt lake research in China. *Acta Geol. Sin.* **2016**, *90*, 2123–2166. (In Chinese). [CrossRef]
15. Yang, J.Y.; Chen, W.Y.; Zhang, Y.; Deng, T.L. A research on the comprehensive utilization channels of intercrystalline brines from Jilaier Lake of Dongtai. *J. Mineral. Petrol.* **1995**, *2*, 81–85. (In Chinese).
16. Wen, J.; Deng, T.L.; Wang, S.Q.; Gao, J.; Guo, Y.F. Caloric evaporation test for the summer salt lake brine in the Dongtaijilaier salt lake. *J. Salt Chem. Ind.* **2011**, *40*, 22–26. (In Chinese).
17. Liang, Q.S.; Han, F.Q. Distribution characteristics of Li content in shallow intercrystalline brine from the Bieletan's northwestern edge in Qarhan Salt Lake area. *J. Salt Lake Res.* **2014**, *22*, 1–9. (In Chinese).
18. Zheng, X.Y.; Zhang, M.G.; Xu, X.; Li, B.X. *China Salt Lake*; Science Press: Beijing, China, 2002. (In Chinese)
19. Xiang, W.; Liang, S.K.; Zhou, Z.Y.; Qin, W.; Fei, W.Y. Extraction of lithium from salt lake brine containing borate anion and high concentration of magnesium. *Hydrometallurgy* **2016**, *166*, 9–15. [CrossRef]
20. Garrels, R.M.; Thompson, M.E. A chemical model for sea water at 25 °C and one atmosphere total pressure. *Am. J. Sci.* **1962**, *260*, 57–66. [CrossRef]
21. Pitzer, K.S. Thermodynamics of Electrolytes. II. Activity and osmotic coefficients for strong electrolytes with one or both ions univalent. *J. Phys. Chem.* **1973**, *77*, 2300–2308. [CrossRef]
22. Harvie, C.E.; Møller, N.; Weare, J.H. The prediction of mineral solubilities in natural waters: The Na-K-Mg-Ca-H-Cl-SO_4-OH-HCO_3-CO_3-CO_2-H_2O system to high ionic strengths at 25 °C. *Geochim. Cosmochim. Acta* **1984**, *48*, 723–751. [CrossRef]
23. Song, P.S.; Yao, Y. Thermodynamics and phase diagram of the salt lake brine system at 298.15 KV Model for the system Li^+, Na^+, K^+, Mg^{2+}/Cl^-, $SO_4{}^{2-}$-H_2O and its applications. *Calphad* **2003**, *27*, 343–352.
24. Zhang, Z.B.; Liu, L.S. Complex chemistry and ocean chemistry. *Chemistry* **1977**, *6*, 25–41. (In Chinese).
25. Turner, D.R.; Whitfield, M.; Dickson, A.G. The equilibrium speciation of dissolved components in freshwater and sea water at 25 °C and 1 atm pressure. *Geochim. Cosmochim. Acta* **1981**, *45*, 855–881. [CrossRef]